IOP Conf. Series: Materials Science and Engineering **1327** (2025) 012149 doi:10.1088/1757-899X/1327/1/012149

Design and construction of an enhanced thermal conductivity measurement set-up in the temperature range of 1.8 K to 50 K at CERN

M Rhandi[1*], S Bischof[1], B Hashinokuti Iwamoto[1], P Borges de Sousa[1] and T Koettig[1]

[1] CERN, CH-1211 Geneva 23, Switzerland

[*]E-mail : maha.rhandi@cern.ch

Abstract. Within the goals of the High-Field Magnet (HFM) program at CERN, ongoing research focuses on achieving magnetic flux densities of up to 16 T using superconducting coils. Understanding the thermal properties of composite materials used as impregnation resins or insulation layers in superconducting magnets is crucial for the design of effective cooling methods. To this end, a new test stand was built at CERN in the Cryogenic Laboratory, to extend the investigation of thermal properties to a lower temperature range compared to the conventional cryocooler-based set-ups stopping at around 3 K, by linking a closed He II circuit to this system. This circuit enables to pre-cool helium gas, then gets it condensed by expansion through a Joule-Thomson valve before it gets pumped continuously via a roots pump, allowing to extend the measurement capabilities down to 1.8 K. The He II circuit is coupled to the cryocooler's cold head via a gas-gap heat switch, enabling the He circuit to be thermally decoupled from the warmer cryocooler head for measurements at the lowest temperature. By varying base temperatures of the experimental platform, providing the cooling power either by the cryocooler or by the He circuit, a steady-state heat flux measurements can be ensured from 1.8 K up to 50 K. This work details the design and construction of this new enhanced test stand for thermal conductivity measurements at a lower temperature range, and its validation by measuring a reference sample.

Keywords: Thermal conductivity, cryocooler, gas-gap heat switch, He II closed-loop circuit

1. Introduction

Understanding thermal properties at cryogenic level is crucial for numerous scientific and technological applications. Knowledge of thermal conductivity, heat capacity, and thermal expansion at low temperatures is essential for designing and optimizing superconducting magnets. Investigating and comprehending thermal properties supports the development of next-generation superconducting magnets. Currently, conventional off-the-shelf cryocooler set-ups for thermal properties investigation stop at around 3 K, whereas specific magnet designs are required to function in the He-cooled regime down to 1.8K. Therefore, a new test stand was constructed at CERN's Cryogenic Laboratory to expand the exploration of thermal properties into lower temperature ranges, achieved by integrating a closed He II circuit into the set-up.

IOP Conf. Series: Materials Science and Engineering **1327** (2025) 012149 doi:10.1088/1757-899X/1327/1/012149

2. Thermal conductivity set-up

2.1 Experimental set-up

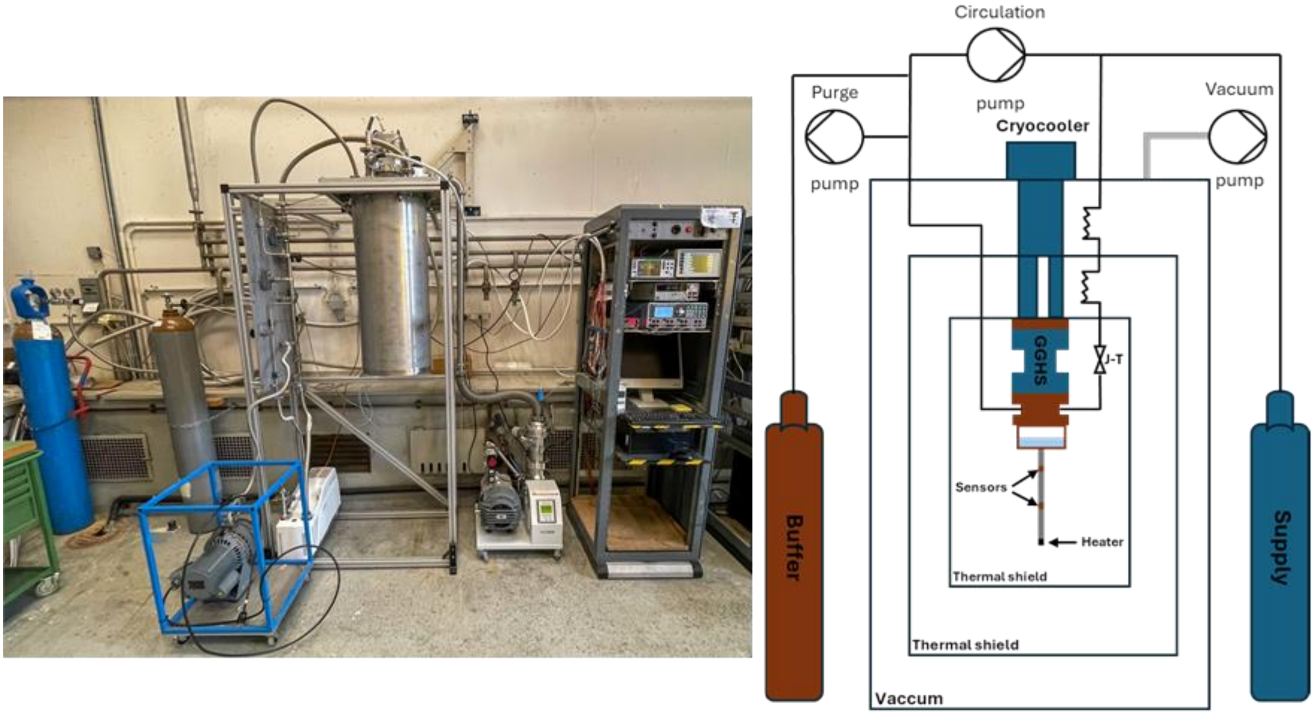

Figure 1. Picture & schematic of the experimental platform for thermal conductivity composed of: helium supply bottle, buffer bottle, pulse tube cryocooler (PTC), vacuum pump, roots pump, purge pump, and data acquisition rack.

Figure 1 displays the different components of the experimental set-up. Figure 2 illustrates the internal components of the cryostat. To enable the study of thermal properties at lower temperatures, the set-up incorporates a closed He II circuit, with a copper pot for helium storage, positioned between the gas gap heat switch (GGHS) and the sample. The He circuit is engineered to generate lower temperatures beyond what the cryocooler can achieve, necessitating the use of the GGHS to thermally insulate the experimental platform with its He pot and the sample from the cryocooler's second stage [1].

A GGHS is a device used in cryogenic applications to control thermal conduction between components or systems. It functions by manipulating the gas density, usually helium, in a narrow gap [2], [3]. The narrower the gap, the more effective it is. This arrangement facilitates an increased conductance in the ON state. Franco et al. [3] highlight the necessity of maintaining a very low gas pressure, approximately 10^{-2} mbar, to achieve optimal thermal insulation in the OFF state. Removing the gas, often through a cryopump, effectively minimizes heat transfer and insulates the components from each other.

When operating the He circuit, the GGHS is switched OFF. The pot is linked to both an inlet helium capillary line and a pumping line. Initially, helium gas enters from the warm side via the capillary tube and undergoes precooling at the first and second stages where the capillaries are wound around the copper flanges. The helium gets precooled with the return flow in the pumping line, facilitated by a counterflow heat exchanger. Inside the pumping line is fitted a compressed copper mesh to improve the exchange process. Following this, the gas passes through a Joule-Thomson valve where it expands and reaches saturation conditions inside the pot. This pot acts as an experimental platform for the sample.

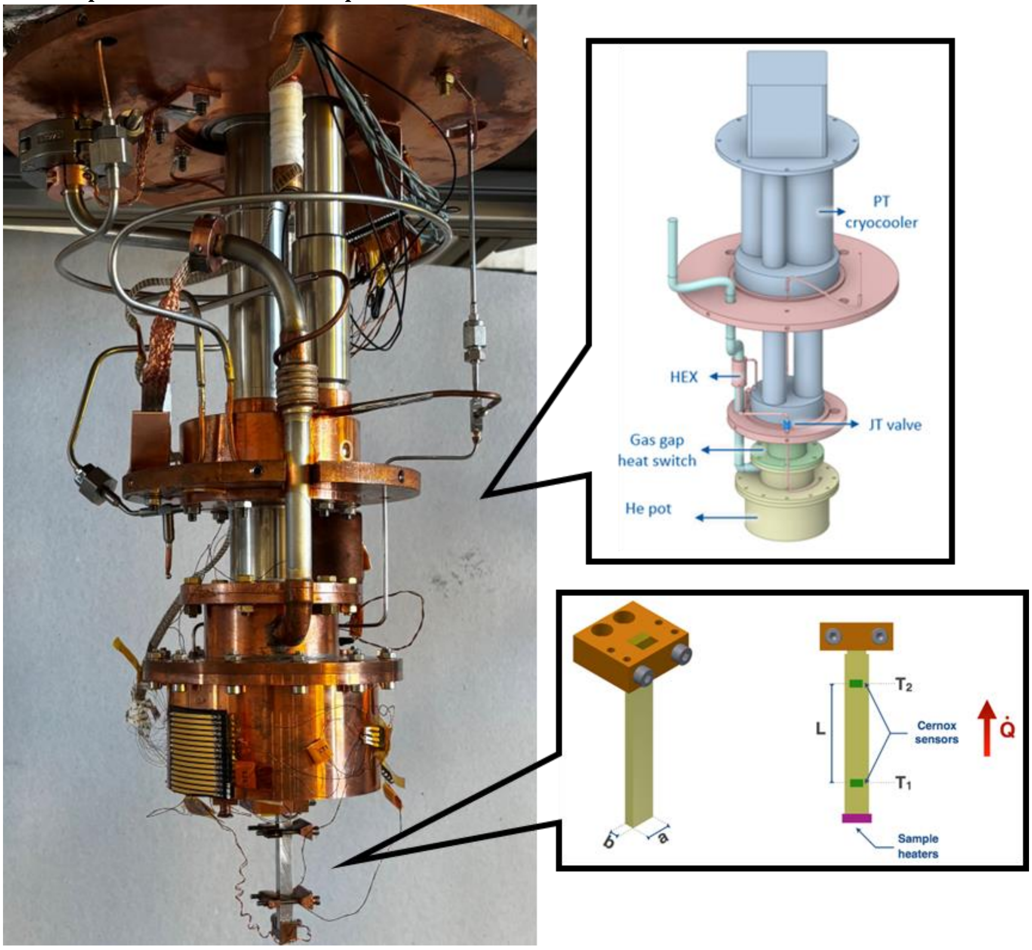

Figure 2. Image of test stand components showing sample integration for thermal conductivity measurements [1].

The first stage of the PTC is used to minimize heat load from all incoming instrumentation wires to the second stage while actively cooling the outer thermal shield to approximately 35 K. Both thermal shields are made of copper cylinder structures and are insulated with a single blanket comprising 10 layers of superinsulation. Heat intercepts are mounted to both the first and second stages of the PTC to thermally stabilize instrumentation wires made of manganin, arranged in a twisted pair configuration. The wire of the electrical heater, which is placed on the bottom end of the sample, are designed with optimized cross-sections of copper or bronze to minimize heat leakage in consideration of the expected thermal conductivity properties of the sample. This design aims to provide the necessary heating power to achieve a temperature gradient of 0.2 K to 0.3 K across the probed sample distance. The objective is to balance the effects of self-heating and thermal conductance of the current-carrying wires, ensuring that the temperature difference between the sample heater and the experimental platform remains less than 0.5 K [4].

IOP Conf. Series: Materials Science and Engineering **1327** (2025) 012149 doi:10.1088/1757-899X/1327/1/012149

In order to validate the set-up, measurements were made using a standard material. The sample was machined from a commercial block of Aluminium alloy 6061 (Al 97.5/Mg 1/Si 0.6/Fe 0.5/Cu 0.4) [5]. The overall length is 70 mm with a cross-sectional area of 50.8 mm^2.

2.2 Thermal conductivity and error calculations

The process for conducting steady-state measurements of a single data point begins with cooling the system to the minimum achievable temperature. A PID controller then regulates the heating power to maintain a constant setpoint temperature, elevating both the platform and the sample to this temperature. During this initial heating phase, no additional heat is applied to the sample by the sample heater (SHT). Following a stabilization period, another PID controls a steady heating power of the SHT located at the bottom of the sample. This creates a temperature gradient across the sample ΔT_{ON}, which is recorded after a specified interval. The sample heater is then deactivated, allowing the sample to cool to the experimental platform temperature. The temperature difference between the two sensors, ΔT_{OFF1} & ΔT_{OFF2}, is monitored over a specific duration following a period of stabilization before and after the SHT is turned on. Ideally, ΔT_{ON} should be 150 mK to 250 mK greater than ΔT_{OFF}, which can be regulated by adjusting the heating power of the electric heater. To reduce potential errors from temperature calibration or parasitic heat loads, the absolute temperature gradient ΔT used to determine thermal conductivity is calculated as $\Delta T = \Delta T_{ON} - \Delta T_{OFF}$, where $\Delta T_{OFF} = \frac{\Delta T_{OFF1} + \Delta T_{OFF2}}{2}$ [6].

This arrangement requires the averaging of the SHT to maintain the constant required temperature. Figure 3 illustrates a heating step undertaken for the measurements of thermal conductivity.

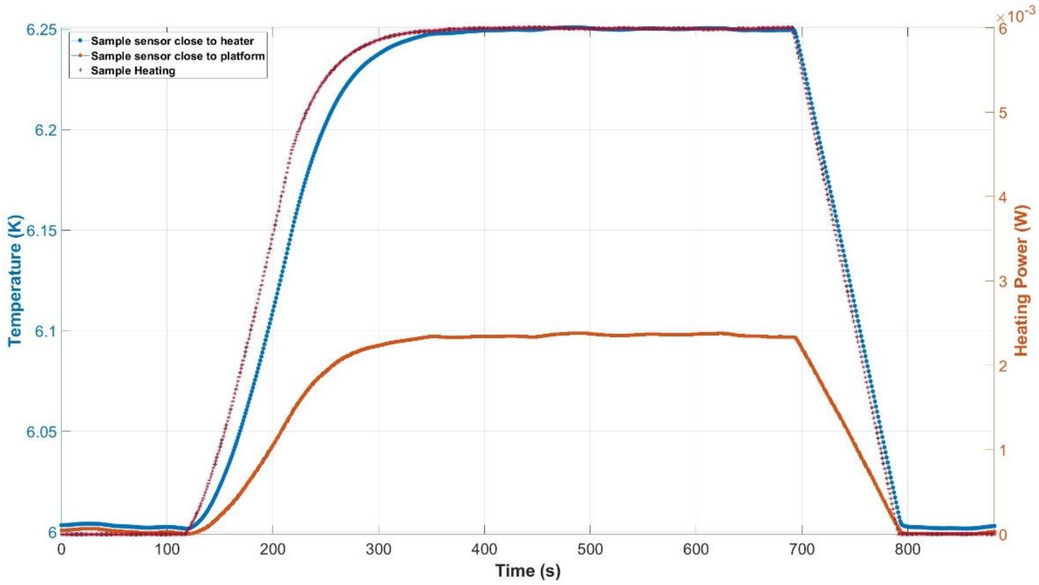

Figure 3. Heating step for the measurements of thermal conductivity.

Using the measured temperature difference ΔT between the two sensors placed on the sample, and the heat load $\dot{Q}$ applied on the bottom of the sample, the thermal conductivity λ is calculated as follows:

$$\lambda = \frac{\dot{Q}L}{A\Delta T} \tag{1}$$

where L is the distance between the two sensors and A is the cross-sectional area of the sample, as shown in Figure 2.

Measurement accuracy estimation covers the precision of the data acquisition of the current sources, the voltmeter, the heater current source, and the sample dimensions uncertainties:

$$\Delta\lambda = \pm\sqrt{\left(\frac{\partial\lambda}{\partial\dot{Q}}\Delta\dot{Q}\right)^2 + \left(\frac{\partial\lambda}{\partial L}\Delta L\right)^2 + \left(\frac{\partial\lambda}{\partial A}\Delta A\right)^2 + \left(\frac{\partial\lambda}{\partial\dot{Q}}\Delta(\Delta T)\right)^2} \tag{2}$$

The relative error for thermal conductivity is Δλ= ±3 %. The absolute error for temperature measurements is estimated at ΔT= 4 mK.

3. Measurement results & discussion

Measurements were performed on a 70 mm Aluminium alloy 6061 sample across temperatures ranging from 3.5 K to 11.8 K. Subsequently, these results were compared with existing literature data to validate the setup. Figure 4 shows the measured thermal conductivity. It consistently increases as the temperature rises, maintaining a monotonous upward trend.

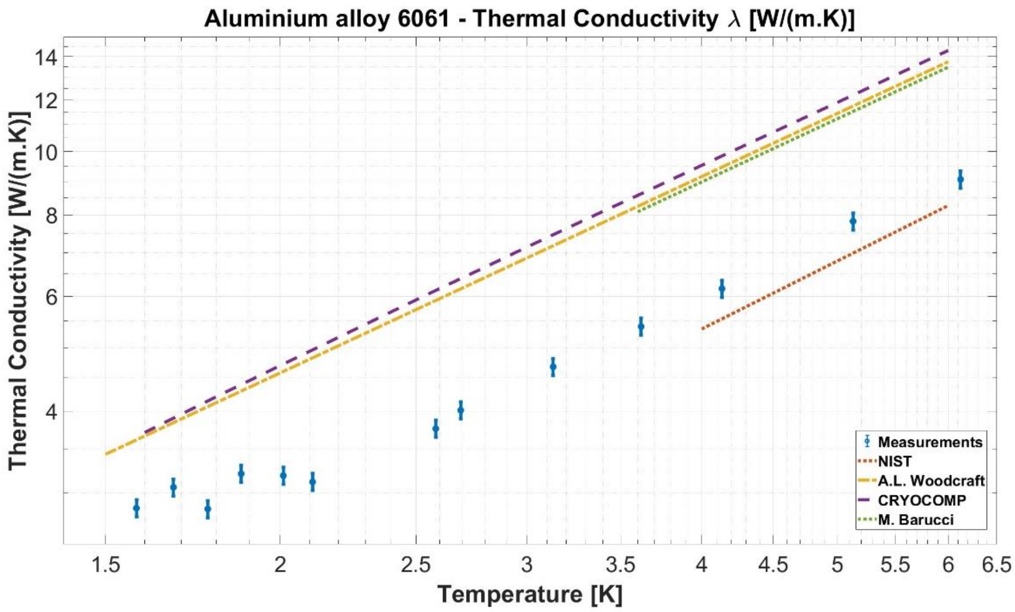

Figure 4. Plot of the thermal conductivity measurement as a function of temperature. Compared to CROYOCOMP [7], NIST [8], Barucci [9], Woodcraft [10] values.

Figure 4 shows also a comparison between the measured thermal conductivity of the aluminum alloy 6061, the NIST [8] database, the Cryocomp [7] engineering database, the empirically calculated values by M. Barucci [9], and the A.L. Woodcraft [10] model values. These measurement values validate the experimental set-up. The data points for the measured thermal conductivity of Aluminum alloy 6061 are positioned between the extrapolated models at lower temperatures.

Specifically, the measurements align above the NIST [8] model, which represents the lower conductivity values, and below the A.L. Woodcraft [10], Cryocomp [7], and M. Barucci [9], which suggest higher conductivity values at these temperatures.

4. Conclusion & perspectives

The experimental platform for measuring thermal conductivity has been designed and constructed at CERN's Central Cryogenic Laboratory. As the set-up continues to undergo commissioning and optimization, efforts are focused on achieving the lowest possible temperatures. Initial testing and validation using a reference sample have yielded promising results, indicating the platform's potential for lower temperature applications. This set-up is well-equipped to enable a detailed exploration of thermal properties of a variety of materials at lower temperatures.

Acknowledgments

The authors would like to thank the High Field Magnet Program for funding the fellowship of Maha Rhandi and the internship of Bruno Hashinokuti Iwamoto. Special appreciation is also extended to Agostino Vacca and Sebastien Prunet for their significant contributions to this project.

References

[1] B. Hashinokuti Iwamoto, "Preliminary design of a 1.8 K thermal conductivity test stand for HFM," CERN, 2868482, 2023. [Online]. Available: http://cds.cern.ch/record/2868482/files/Bruno_Iwamoto_CERN_report.pdf?version=1

[2] X. Xi, B. Yang, Z. Gao, L. Chen, Y. Zhou, and J. Wang, "Helium gas-gap heat switch for Sub-Kelvin refrigeration system," *IOP Conf. Ser.: Mater. Sci. Eng.*, vol. 1240, no. 1, p. 012023, May 2022, doi: 10.1088/1757-899X/1240/1/012023.

[3] J. Franco, B. Galinhas, P. B. D. Sousa, D. Martins, I. Catarino, and G. Bonfait, "Building a Thinner Gap in a Gas-Gap Heat Switch," *Physics Procedia*, vol. 67, pp. 1117–1122, 2015, doi: 10.1016/j.phpro.2015.06.173.

[4] T. Koettig *et al.*, "Thermal conductivity measurements of impregnated Nb_3Sn coil samples in the temperature range of 3.5 K to 100 K," *IOP Conf. Ser.: Mater. Sci. Eng.*, vol. 171, p. 012103, Feb. 2017, doi: 10.1088/1757-899X/171/1/012103.

[5] "Good Fellow, 6061 aluminium foil." [Online]. Available: https://www.goodfellow.com/fr/material/alloys/aluminium-6000-series-alloys/6061-aluminium-foil

[6] P. Borges de Sousa and T. Koettig, "Thermal Conductivity of impregnated Nb3Sn coil samples 11 TESLA DIPOLE SAMPLES: #8: S-2 GLASS 636 11 TEX REACTED WITHOUT CERAMIC BINDER AND IMPREGNATED IN CTD-101K RESIN, 7 MM-THICK SAMPLE," 2042486, Nov. 2017. [Online]. Available: https://edms.cern.ch/ui/file/2042486/1/Report_11T_dipole_sample_8.pdf

[7] "Cryocomp, Eckels Engineering, v. 3.06. Cryodata Inc., Florence, SC 29501, USA, CRYOCOMP® is a database code of the state and thermal properties for technical materials."

[8] Y. S. Touloukian, "NIST, Thermal Conductivity, Thermal Properties Database for Materials at Cryogenic Temperatures. Ed. Holly M. Veres. Volume 1. Recommended values of the Thermophysical Properties of eight Alloys, Major Constituents and their Oxides,." [Online]. Available: https://www.nist.gov/mml/acmd/aluminum-6061-t6-uns-aa96061

[9] M. Barucci, L. Risegari, E. Olivieri, E. Pasca, and G. Ventura, "ALUMINIUM ALLOYS FOR SPACE APPLICATIONS: LOW TEMPERATURE THERMAL CONDUCTIVITY OF A6061-T6 AND A1050," in *Astroparticle, Particle and Space Physics, Detectors and Medical Physics Applications*, Villa Olmo, Como, Italy: WORLD SCIENTIFIC, Jul. 2004, pp. 541–545. doi: 10.1142/9789812702708_0079.

[10] A. L. Woodcraft, "Predicting the thermal conductivity of aluminium alloys in the cryogenic to room temperature range," *Cryogenics*, vol. 45, no. 6, pp. 421–431, Jun. 2005, doi: 10.1016/j.cryogenics.2005.02.003.